# ENERGETICALLY COMPETITIVE GROWTH PATTERNS OF SILICON CLUSTERS: QUASI-ONE-DIMENSIONAL CLUSTERS VERSUS DIAMOND-LIKE CLUSTERS

P.L. Tereshchuk, Z.M. Khakimov

Institute of Nuclear Physics of Uzbekistan Academy of Sciences, Tashkent 702132, Uzbekistan;

khakimov@inp.uz

M.T. Swihart

Department of Chemical and Biological Engineering

University at Buffalo (SUNY), Buffalo, NY 14260-4200, USA

ABSTRACT

Silicon clusters with a diamond-like core and energetically competitive non-diamond clusters were comparatively studied using the nonconventional tight-binding molecular dynamics simulation method. Non-diamond clusters were constructed according to a quasi-one-dimensional pentagon-based regular growth pattern. A non-trivial competition between surface and core reconstructions in the clusters, in order to reach energetically favorable atomic arrangements, was observed. This prevents unlimited growth via the one-dimensional pattern. Starting from $Si_{43}$, there was substantial deviation from the stacked pentagon motif, and for $Si_{61}$ one end of these clusters became almost two-dimensional. The structure of clusters with a diamond-like core was subject to substantial reconstruction for the cluster sizes considered (≤ 71 atoms). By extrapolating the present results, a lower bound for the transition from non-diamond structure to diamond-like structure is estimated to be 115 atoms.

PACS numbers: 71.15.Nc, 61.46.+w, 73.22.-f

## 1. Introduction

Nanometer-size silicon clusters have been attracting much attention since the observation of efficient luminescence from porous silicon[1], due to their potential use as light emitters in displays or general illumination and as fluorescent probes for bioimaging. To date, Si nanoparticles ranging from 1 to 5 nm in diameter have been prepared by a variety of methods[2-7] and found to exhibit photoluminescence at wavelengths ranging from blue to the near infrared. The core of luminescent Si nanoparticles is commonly presumed to be diamond-like as in bulk silicon, with each silicon atom surrounded symmetrically by four other Si atoms that form a perfect tetrahedron. The smallest (1 nm in diameter) model of luminescent Si particles is an H-terminated, reconstructed $Si_{24}$ cluster cage with one silicon tetrahedron in the interior[8], that is $Si_5Si_{24}H_{24}$. The perfect diamond-like coordination of Si atoms, at least up to this size, can by stabilized only by termination of surface dangling bonds of Si atoms by hydrogen or other atomic or molecular species. Bare clusters, containing up to seven Si atoms are compact clusters[9], while larger clusters tend to have prolate shapes[10]. The particles are again spherical for numbers of atoms in the range[10] from 20 to 30, but they have little resemblance to the bulk silicon structure. Moreover, globally minimum energy clusters that differ in size by only by one atom may have quite different structures.

In spite of the large number of calculations performed by a variety of state-of-the-art ab initio methods, which have somewhat clarified these and other peculiarities of the structural changes in silicon clusters with increasing size, fundamentally interesting and long-standing questions regarding the "non-diamond cluster structure to diamond structure transition" for bare silicon clusters still remain unanswered. In particular, the critical cluster size at which such a transition occurs has not been conclusively determined. Simulation of small clusters of 10 or fewer silicon atoms using pseudopotential-density-functional techniques and extrapolation of the results to large

clusters[11] led to an early estimate of over 4000 atoms for the critical size for this transition. In contrast, early tight-binding calculations[12] estimated this size to be only 50 silicon atoms. More recent tight-binding calculations[13] give a somewhat intermediate result for the critical size, 400 atoms. It is interesting to note that there are scanning probe experiments that seem to support both small[14] and large critical sizes[15]. Therefore work remains to be done in order to achieve a consensus on the critical cluster size for the nondiamond to diamond transition for bare silicon clusters. From a theoretical point of view, the exponential growth of the number of possible isomers of clusters with increasing size, even provided with tremendous computational resources, makes testing and comparing them directly unrealistic, especially by ab initio methods. On the other hand, conventional tight-binding models do not have the accuracy required to reliably determine small energy differences between dissimilar large clusters.

Recently we developed[16] and parameterized the non-conventional tight-binding method (NTB) for simultaneously describing the geometry and cohesive and spectroscopic energies (ionization potentials and electronic affinities) of silicon clusters with accuracy comparable to that of the state-of-the-art ab initio methods. We also proposed[16] a regular (smooth), quasi-one-dimensional growth pattern of silicon clusters that appears to be energetically competitive with the irregular growth pattern established by ab initio calculations[10] in the range of clusters sizes up to 20 atoms. Such a cluster growth pattern can be continued infinitely in one direction, provided that there are no significant distortions or other energetically more favorable growth channels. One possible competitive growth channel, of course, would consist of clusters with a diamond-like core. Suggesting that the clusters from this growth pattern can effectively represent the lowest-energy non-diamond structures for larger clusters as well makes it feasible to identify the transition of silicon clusters from a non-diamond structure to that with a diamond-like core by comparing the dependence of binding energy on size for these two classes of clusters.

In this paper we first demonstrate limiting factors for the growth of silicon clusters according to the regular one-dimensional pattern, determining a cluster size up to which the clusters' cohesive energy increases. Then, clusters in this size range with a diamond-like core are comparatively studied. The next section briefly describes computational details and the approach used for constructing clusters. The results obtained are discussed in the third section. The last section summarizes the key findings.

## 2. Computational details

The total energy functional of NTB is[16]

$$E_{tot} = \sum_{\mu}\sum_{\nu>\mu} \frac{Z_{\mu}^{scr} Z_{\nu}^{scr}}{R_{\mu\nu}} + \sum_{\mu}\sum_{\nu>\mu} \frac{Q_{\mu} Q_{\nu}}{R_{\mu\nu}} + \sum_{\mu}\sum_{\nu>\mu}\sum_{i}\sum_{j} P_{\mu i,\nu j} H_{\mu i,\nu j} + \sum_{\mu} (E_{\mu} - E_{\mu}^{0}), \quad (1)$$

where $R_{\mu\nu}$ is the internuclear distance,

$$Z_{\mu}^{scr} = Z_{\mu}^{scr}(R_{\mu\nu}, \{N_{\mu i}^{0}\}) = Z_{\mu} - \sum_{i} N_{\mu i}^{0} [1 - a_{\mu i} \exp(-\alpha_{\mu i} R_{\mu\nu} / R_{\mu i}^{0})], \quad (2)$$

$$Q_{\mu} = Z_{\mu}^{scr}(R_{\mu\nu}, \{N_{\mu i}^{0}\}) - Z_{\mu}^{scr}(R_{\mu\nu}, \{N_{\mu i}\}), \quad (3)$$

are screened nuclear and nonpoint ionic charges, respectively; $Z_{\mu}$ is the charge of the $\mu^{\text{th}}$ nucleus (or nucleus plus core electrons); $R_{\mu i}^{0} = n_{\mu i} / \xi_{\mu i}^{0}$ is the most probable distance between the $i^{\text{th}}$ electron and the corresponding $\mu^{\text{th}}$ nucleus, $n_{\mu i}$ and $\xi_{\mu i}^{0}$ are the principal quantum number and Slater exponent of the $i^{\text{th}}$ AO centered at the $\mu^{\text{th}}$ nucleus; $E_{\mu}^{0}$ and $E_{\mu}$ are the total energies of individual atoms in non-interacting and interacting systems characterized by sets of occupancy numbers $\{N_{\mu i}^{0} \equiv P_{\mu i,\mu i}^{0}\}$ and $\{N_{\mu i} \equiv P_{\mu i,\mu i}\}$ and energies $\{E_{\mu i}^{0}\}$ and $\{E_{\mu i}\}$ of valence AOs, respectively; $\alpha$ and $a$ are fitting parameters.

AOs are presumed to be orthogonal and a secular equation $\sum_{vj}(H_{\mu i,vj} - \varepsilon\delta_{\mu i,vj})C_{vj} = 0$ is solved self-consistently to obtain electronic spectra $\{\varepsilon_k\}$ and AO expansion coefficients $\{C_{vj}(k)\}$ of the molecular orbitals (MO) of the system. Self-consistent calculations are performed by iterative recalculation of diagonal elements of the Hamiltonian matrix elements $H_{\mu i,vj}$ using the dependence of the bond-order matrix and AO occupancy numbers $N_{\mu i} \equiv P_{\mu i,\mu i}$ on $C_{vj}(k)$.

For other formulae and details of NTB see Ref.[16]. Here we should note the following. NTB uses a total energy functional that is different in form from commonly used TB energy functionals. NTB uses a new definition of the repulsive energy term with simple physical content; it is the sum of the repulsion energy between nuclei and half of the attraction energy of electrons to "foreign" nuclei. In NTB, this term (the first term in (1) in the non-self-consistent calculation case), unlike that in traditional TB, does not contain the complex interatomic electron-electron interaction energy even implicitly, and thus can be represented more reliably by short-range pairwise functions of interatomic distances. The accurate and detailed parameterization of ionization and promotion energies of atoms and ions is another principal difference between NTB and traditional TB models. This allows the method to account adequately for the majority of correlation effects in multiatomic systems as well. Using these features, we have been able to extend NTB far beyond the capabilities of traditional TB for describing geometry, cohesive energy, ionization potentials, and electron affinities of bare silicon[16] cluster containing up to 20 atoms, as well as atomization energies of more than 130 silicon-hydrogen[17] clusters with accuracy comparable to state-of-the-art ab initio methods. Furthermore, NTB gave good predictions of bulk silicon properties (lattice constant, cohesive energy, band gap, etc.)[16] using a parameterization based entirely on properties of atoms and small clusters, unlike traditional TB methods that use the bulk properties in the parameterization. This

increases our confidence in property predictions for clusters much larger than those used in the parameterization.

The regular growth pattern considered in Ref.[16] starts from $Si_7$ with a bicapped pentagon geometry. It reaches icosahedral $Si_{13}$ by sequential addition of Si atoms to complete another pentagon above $Si_7$ then capping this pentagon by a sixth Si atom (Figure 1). Note this pattern provides at least four bonds for each Si atom, except in clusters of $Si_{14+6n}$ ($n$=0,1,2…), in which there is one three-coordinated atom. The clusters $Si_{13+6n}$ with completed and capped pentagons, which can be obtained by sequentially adding the capped pentagonal motif to $Si_7$, $Si_{13}$, $Si_{19}$, etc. (Figure 1), are "magic" ones that have higher cohesive energies than neighboring members of the series. Thus, clusters from this series were chosen for simulation and comparison to the diamond-like clusters.

For comparison, we consider a few clusters of similar size with a diamond-like core. Namely, we start from three prototype clusters (Figure 2) cut from the bulk silicon structure, consisting of 29, 38 and 59 atoms, respectively. The large number of surface dangling bonds on these clusters makes them energetically unfavorable compared to compact or overcoordinated structures. The most undesirable surface atoms in the clusters shown in Figure 2 are those with two dangling bonds. To eliminate them we simply form dimers or trimers from them; the former are well-known structures on the (100) surface of bulk silicon and seem to be necessary even in the case of small hydrogen-saturated clusters[8]. We also created another set of clusters, embedding additional atoms into the surface of the prototype clusters in a such way that each of them occupied a position that would correspond to a tetrahedral interstitial position in bulk silicon (Figure 2). This increases the coordination number of surface atoms and is therefore expected to increase the cohesive energy of clusters with large surface to volume ratio. After optimizing the geometry of these clusters, we

derived from them a few more clusters, removing some surface atoms in possibly strained configurations. Optimization of all cluster geometries was performed by a computational approach[16] that combines NTB with molecular-dynamics using an accurate algorithm[18] for integration of the equations of motion.

## 3. Results and Discussion

**Pentagon-based one-dimensional clusters.** Figures 3 and 4 depict the geometries of optimized clusters from the regular growth pattern, containing up to 61 atoms. As shown there, the larger clusters are significantly distorted and do not perfectly follow the growth pattern illustrated in Figure 1. The distortion increases with increasing cluster size, due to accumulation of strain in the bonds between the silicon atoms along the central axis of the clusters. These atoms are shown as pink balls for clarity. In the idealized clusters, these bonds are much shorter than expected for their given coordination numbers, and were closer to the bond length in $Si_2$ (~2.25 Å). Such short distances were forced by the binding of surface atoms from different pentagons. The distances between these atoms, unlike the distances between atoms on the central axis, was as expected (≥ 2.35 Å) given their coordination numbers (≥ 4).

Thus, the competition between increasing the cluster cohesive energy by establishing optimal bond lengths and angles for the surface atoms vs. decreasing of this energy due to constraint of the atoms along the cluster central axis to sub-optimal bond lengths, governs behavior of this non-diamond one-dimensional growth channel. The shrinking of the clusters' surface along the growth direction forces the atoms on the central axis closer to each other. To diminish their repulsive interactions, these atoms deviate from their ideal locations in a straight line on the cluster axis. As a result, they tend to form a zigzag, which, in turn, leads to distortion of the pentagons formed by

surface atoms. However, there is limited space for the formation of this zigzag pattern within the interior of small clusters. This causes very strong distortion of one end of the cluster $Si_{25}$, preventing this end from growing further via the capped pentagon motif. In the larger clusters, this end then serves as sink for accommodating further bond strain. In the $Si_{49}$ cluster, it incorporates a two-dimensional four-atom motif within its interior. In the $Si_{61}$ cluster, this end has become almost fully two-dimensional (Figure 4). This cluster has the largest binding energy per atom (4.5 eV, which is ~0.13 eV lower than the value for bulk silicon) among clusters considered.

The further addition of atoms to the above clusters, of-course not necessarily according to the pattern shown in Figure 1, would be of particular interest, because in this way one may be able to observe a transformation of the above clusters to three dimensional ones with a diamond-like core. However, simulations performed for the $Si_{67}$ cluster constructed according to the pattern in Figure 1 and for several other clusters with Si atoms added to the $Si_{61}$ cluster at peripheral positions all predicted smaller binding energies per atom than that obtained for $Si_{61}$. Thus, $Si_{61}$ seems to be an end-point of sorts for this growth pattern, where a maximum in binding energy per atom is achieved.

**Clusters with an initially diamond-like core.** The optimized geometries of clusters that initially had a diamond-like core are depicted in Figure 5. Three additional derived geometries are also shown, based on removal of vertex atoms from optimized clusters. One can see significant shrinking of the surface formed by dimerized atoms in the cluster Si29D; the distance between them and the central atom is 3.43 Å in the optimized geometry, which is significantly shorter than the second-nearest-neighbor distance in bulk silicon, 3.93 Å. Bond distances between the dimerized atoms and neighboring surface atoms are only 2.266 Å. Other bonds are ~2.31 Å, and form a nearly ideal diamond-like structure. In the overcoordinated cluster Si29E6 the central atom completely lost its tetrahedral coordination. In the optimized structure, it has octahedral coordination due to inversion of the positions of the six embedded atoms and the four initial nearest-neighbor atoms of

the central atom. The distance between the central atom and its six octahedrally-coordinated neighbors is only 2.245 Å, while the length of other bonds is between 2.345 Å and 2.368 Å.

The dimerized cluster Si38D primarily showed surface reconstruction, but this reconstruction was significant and led to the formation of capped pentagon motifs on the surface (Figure 5). The latter was possible because of strong buckling of dimers, such that one of the atoms in each pair became a 3-coordinated vertex atom. The distance between the two central atoms is 2.293 Å, and the distance between them and their other nearest-neighbors is slightly larger, 2.305 Å. The bond distances between the peripheral atoms range from slightly smaller, 2.278 Å, to somewhat larger, up to 2.40 Å. The largest bond distances are between the vertex atoms and their neighbors. We derived cluster Si32S from Si38D by removing the six three-coordinated vertex atoms and optimizing the geometry of the resulting cluster. This increased the cohesive energy per atom, in spite of the decrease in number of atoms. All bond distances became larger than 2.32 Å, and the largest one, 2.46 Å, was between the two central atoms.

In the cluster Si38E6 one can see both strong surface (Figure 5) and core (Figure 6) reconstruction. Again one can see capped pentagon motifs and 3-coordinated vertex atoms. In this cluster, the pairs of outermost atoms that initially had two dangling bonds apiece were displaced so that one member of each pair became a three-coordinated vertex atom, while the other became the capping atom of a capped pentagon. The two central atoms lost their tetrahedral coordination. The distance between them is 2.41 Å, while the distance between them and their other first neighbors is 2.48 Å. The shortest bond distance between peripheral atoms is 2.323 Å. In the cluster Si38S smoothened by removing the 6 vertex atoms from Si38E6, the cohesive energy per atom again increases. The main geometrical change is that distance between two central atoms became 2.322 Å, which almost coincides with the shortest bond distance in the cluster, 2.315 Å.

In the trimerized cluster Si59T, the distance between the central atom and its first neighbors is 2.309 Å. Other bond distances range from 2.32 Å to 2.52 Å. Here on the surface region (Figure 5) one can recognize a somewhat modified fragment of clusters from the pentagon-based one dimensional pattern (Figures 3 and 4), which causes large bond distances. Cluster Si59E12 and its derivative, Si65S, also have such a fragment, but larger in size and with a different orientation. Note, however, in all three clusters (Si59T, Si59E12, Si65S) these fragments do not involve internal axial atoms like those in the clusters shown in Figures 3 and 4. In the optimized geometry, the central atom in each trimer (Si59T, see Figure 2) became embedded into the cluster (Figure 5) after geometry optimization. As a result, the final structure represents a combined realization of the two types of cluster construction described in the previous section. Surface smoothing has a strong influence on internal bond distances in the case of Si59E12 and Si65S as well. The distance between the central atom and its first neighbors in the latter (2.373 Å) became noticeable larger than that in the former (2.279 Å). However, the distance between the first and second neighbors of the central atom is ~2.28 Å in both clusters.

Dimerized clusters have smaller cohesive energies per atom than other clusters. However, the trimerized cluster that exhibits a combination of the two growth motifs has the largest cohesive energy per atom, 4.355 eV. This was the largest among all initially diamond-like clusters considered, including those with a larger number of atoms. From Figure 6 one can conclude that the first set of clusters, with dimerized or trimerized surface atoms (Si29D, Si38D, Si59T), can be considered as representatives of clusters with a diamond-like core. The other two sets of clusters, (Si29E6, Si38E6, Si59E12) and (Si32S, Si38S, Si65S), can not be considered as such because of the qualitative deviation of their core from the tetrahedrally coordinated diamond structure. Moreover, energies of clusters from these two sets (Figure 5) do not show any regular dependence on the number of atoms in the cluster.

The largest cohesive energy per atom (4.355 eV) for representative diamond-like clusters is still smaller than that for representative non-diamond clusters (4.50 eV), so that the non-diamond cluster structures remain energetically preferable over the entire size range considered here. Larger (perhaps, much larger) diamond-like clusters must be simulated in order to conclusively identify a size at which the diamond-like clusters become energetically preferable. Based on the results obtained here, the surface regions of such larger clusters are expected to be reconstructed such that they consist of pentagon-based fragments attached to a core fragment of diamond-like structure. From this point of view, it is rational to start from clusters constructed as linked pentagon-based fragments and ideal diamond-structures, and not from dimerized or trimerized structures like in Figure 2. Such an approach may also help to avoid the problem of being trapped by intermediate structures.

**HOMO-LUMO gap**. The estimation of the HOMO-LUMO gap for small non-saturated silicon clusters by scanning tunneling spectroscopy measurements[19] found two distinct size regions: between 2.5 and 15 Å, clusters show energy gaps up to 0.45 eV, while above 15 Å only zero (or almost zero) gaps were observed. At the same time, in the first size region the energy gap does not monotonically increase with decreasing size, and there are clusters with zero gaps in this region as well. The HOMO-LUMO gap of the clusters calculated here (Table 1 and 2), for clusters in the small size regime, are in qualitative agreement with this experiment, reflecting non-regularity of gap with cluster size and a similar maximum gap of 0.407 eV (Table 1) or 0.523 eV (Table 2). The zero (or almost zero) gaps that particularly occur for large clusters indicate another possibility for obtaining favorable diamond-like clusters, via disordering and amorphization of their surface. The mixing of close HOMO and LUMO states, the number of which in general increases with cluster size, can initiate a great variety of distortions. Indeed, depending on the initial geometry, in the case of Si38E6 we had convergence problems in self-consistent calculations because of such mixing.

The calculations were continued, in spite of some instabilities of the molecular-dynamics trajectories, and eventually full convergence was reached for a fully disordered structure with only overcoordinated atoms. The cohesive energy per atom for this cluster was only 0.04 eV smaller than the cluster with closest size, $Si_{43}$, from the one-dimensional growth pattern. Thus, at these small sizes, fully disordered structures can also be energetically competitive.

Although calculations on larger clusters are clearly needed to definitively identify a transition from non-diamond-like to diamond-like clusters, we can still estimate a lower bound for this transition point based on the results presented above. In order to do this, we approximated the cohesive energy per atom of representative clusters by the following function

$$E_{coh} = E_{\infty} - E_{\infty} / \{1 + [(N-1)/\widetilde{N}]^{q}\},$$

where $N$ is number of atoms in the cluster, and $E_{\infty}$ is a saturation value of cohesive energy per atom when $N \to \infty$. $E_{\infty}$, $\widetilde{N}$ and $q$ are fitting parameters that were obtained by matching the cohesive energies of three clusters from each series. Clusters Si29D, Si38D and Si59T, as discussed above, represent diamond-like clusters. For the non-diamond clusters, we accounted for clusters without a two-dimensional end, that is, only up to cluster $Si_{43}$ (Figure 3). Our estimation is expected to be a lower bound for the non-diamond to diamond transition, since distortions from the one-dimensional growth pattern may lead to higher cohesive energies, as observed for $Si_{49}$, $Si_{55}$, and $Si_{61}$ clusters. We obtained following values of fitting parameters

$$E_{\infty} = 4.573 \text{ eV},\ \widetilde{N} = 9.852,\ q = 1.672$$

for diamond-like clusters and

$$E_{\infty} = 4.515 \text{ eV},\ \widetilde{N} = 5.150,\ q = 1.778$$

for non-diamond clusters (Figure 7).

It is interesting to note that the saturation value 4.573 eV of cohesive energy per atom for diamond-like clusters almost coincides with bulk cohesive energy obtained by NTB[16], 4.582 eV, and it is higher than that for non-diamond clusters. Thus, according to our calculations, a lower bound of critical cluster size for the non-diamond to diamond transition can be estimated to be about 115 atoms (Figure 7), and the binding energy per atom of clusters at this transition point is about 4.50 eV. This also coincides with the largest binding energy of non-diamond clusters, achieved for $Si_{61}$.

## 4. Conclusion

In summary, silicon clusters with a diamond-like core and non-diamond cluster structures were simulated and compared using the nonconventional tight-binding molecular dynamics simulation method[16]. Non-diamond clusters were constructed according to a pentagon-based regular growth pattern proposed previously[16]. For clusters with a diamond-like core, energetically unfavorable dangling bonds on their surface were partially eliminated by dimerization (trimerization) of Si atoms with two dangling bonds and/or overcoordination of surface atoms. A non-trivial competition of surface and core reconstruction in the clusters, in order to reach energetically favorable atomic arrangements, was observed, accompanied by distortions and partial amorphization of the initially highly regular and symmetric structures. This eventually restricts the one-dimensional growth of clusters of the regular growth pattern from both geometrical and energetic points of view. The maximum cluster size for this pattern is about 61 atoms. However, starting from the cluster $Si_{49}$, one end of these clusters became rather two-dimensional. In the range of cluster sizes ($\leq$ 71 atoms) considered, clusters with a diamond-like core are energetically unfavorable compared to representative non-diamond clusters from the regular, one-dimensional growth pattern. Optimized geometries of the structures with a diamond-like core were sensitive to

the initial surface reconstruction model. In many cases, these cluster geometries converged to structures that no longer contained a diamond-like core. The results obtained here can be extrapolated to estimate a lower bound for the transition from the non-diamond structure to diamond-like structure of about 115 atoms for pure silicon clusters.

**Acknowledgements**

The research described in this publication was made possible in part by Uzbek Academy Sciences Fund for Supporting Fundamental Research (No 6-06), and the U.S. National Science Foundation (grant CTS-0500249). PLT was supported by CRDF ANNJSF grant (No UZC1-2671-TA-05).

**References**

1. L.T. Canham, Appl. Phys. Lett. **57**, 1046 (1990).
2. G. Belomoin, J. Therrien, *et al.*, Appl. Phys. Lett. **80**, 841 (2002).
3. M.V. Wolkin, J. Jorne, *et al.*, Phys. Rev. Lett. **82**, 197 (1999).
4. J.P. Wilcoxon, G.A. Samara, and P.N. Provencio, Phys. Rev. B **60**, 2704 (1999).
5. J.A. Carlisle, M. Dongol, *et al.,* Chem. Phys. Lett. **326**, 335 (2000).
6. D.S. English, L.E. Pell, *et al.,* Nano Letters **2**, 681 (2002).
7. F. Hua, M.T. Swihart, E. Ruckenstein, Langmuir **21**, 6054 (2005).
8. E. Draeger, J.C. Grossman, A.J. Williamson, G. Galli, J. Chem. Phys. **120**, 10807 (2004).
9. K. Raghavachari and C. M. Rohlfing, J. Chem. Phys. **89**, 2219 (1988); ibid **96**, 2114 (1992).
10. K. M. Ho, A.A. Shvartsburg, B. Pan, Z. Y. Lu, C. Z. Wang, J. G. Wacker, J. L. Fye, M. F. Jarrold, Nature (London) **392**, 582 (1998).
11. D. Tomanek and M. A. Schluter, Phys. Rev. B **36**, 1208 (1987).

12. J. R. Chelikowsky, Phys. Rev. Lett. **60**, 2669 (1988).

13. D. K. Yu, R. Q. Zhang, and S. T. Lee, Phys. Rev. B **65**, 245417 (2002).

14. P. Mélinon, P. Kéghélian, B. Prével, V. Dupuis, A. Perez, B. Champagnon, Y. Guyot, M. Pellarin, J. Lermé, M. Broyer, J. L. Rousset, and P. Delichére, J. Chem. Phys. **108**, 4607 (1998).

15. B. Marsen, M. Lonfat, P. Scheier, and K. Sattler, Phys. Rev. B **62**, 6892 (2000).

16. Z.M. Khakimov, P.L. Tereshchuk, N.T. Sulaymanov, F.T. Umarova, M.T. Swihart, Phys. Rev. B **72**, 115335 (2005); Z.M. Khakimov, J. Physics: Conf. Ser. **29**, 177 (2006).

17. Z.M. Khakimov, P.L. Tereshchuk, N.T. Sulaymanov, F.T. Umarova, A.P. Mukhtarov, M.T. Swihart, Non-conventional tight-binding molecular dynamics simulation of bare silicon and silicon-hydrogen clusters. ECS Transactions, ***in press*** (2006).

18. Z.M. Khakimov, Comput. Phys. Comm. **147**, 731 (2002).

19. B. Marsen, M. Lonfat, P. Scheier, K. Sattler, Phys. Rev. B **62**, 6892 (2000).

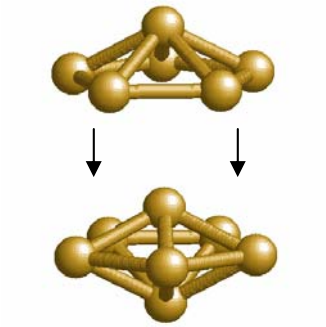

**Figure 1.** Starting cluster (below) and repeating unit (top) of the pentagon-based one-dimensional growth pattern[16].

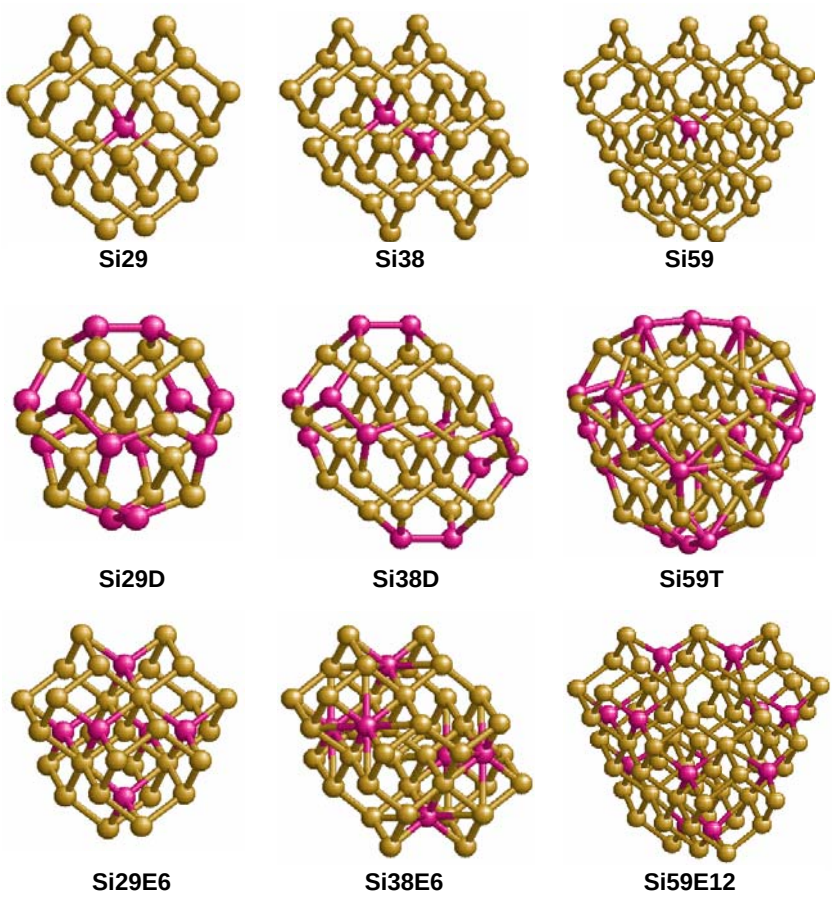


**Figure 2.** (Color online) Three prototypical diamond-like clusters: $Si_{29}$, centered on a single atom (Si29), $Si_{38}$, centered on a Si-Si bond (Si38), and $Si_{59}$, centered on a single atom (Si59), respectively, that were used as the basis for clusters with a diamond-like core. Also shown are the corresponding idealized structures with dimerization (Si29D, Si38D) or trimerization (Si59T) of the surface silicon atoms that have two dangling bonds each, and clusters with additional atoms embedded beneath the surface to increase the coordination number of surface atoms (Si29E6, Si38E6, Si59E12). The atoms of interest in each case (central atom(s) in top row, dimerized or trimerized atoms in second row, and embedded atoms in third row) are shown as pink balls.

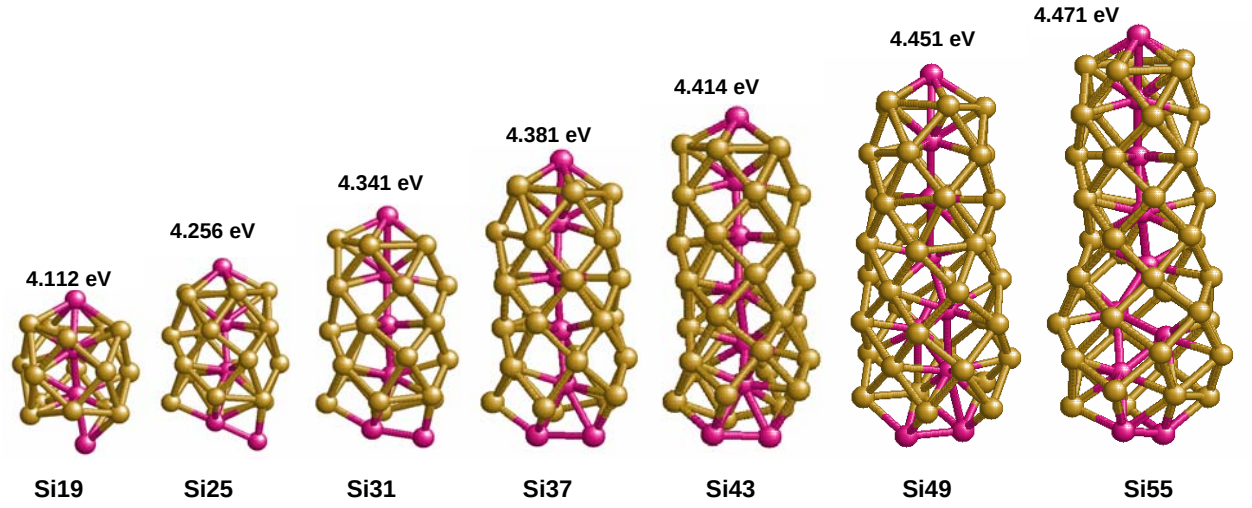


**Figure 3.** (Color online) Optimized geometries of quasi-one-dimensional non-diamond clusters (see also Figure 4). The cohesive energy per atom for each cluster is also given.

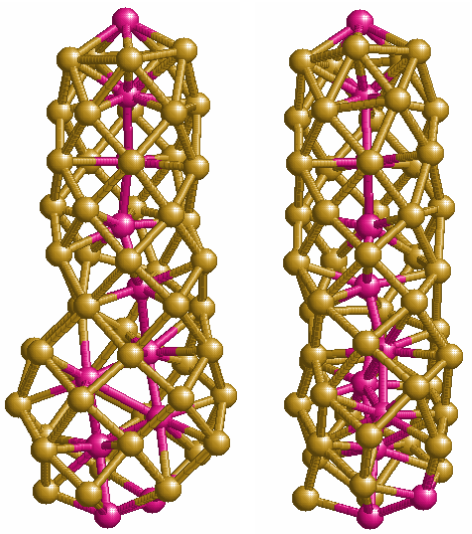

**Figure 4.** (Color online) Two views of the optimized geometry of the $Si_{61}$ cluster (cohesive energy per atom is 4.50 eV) showing the quasi-two-dimensional character of one end of the cluster.

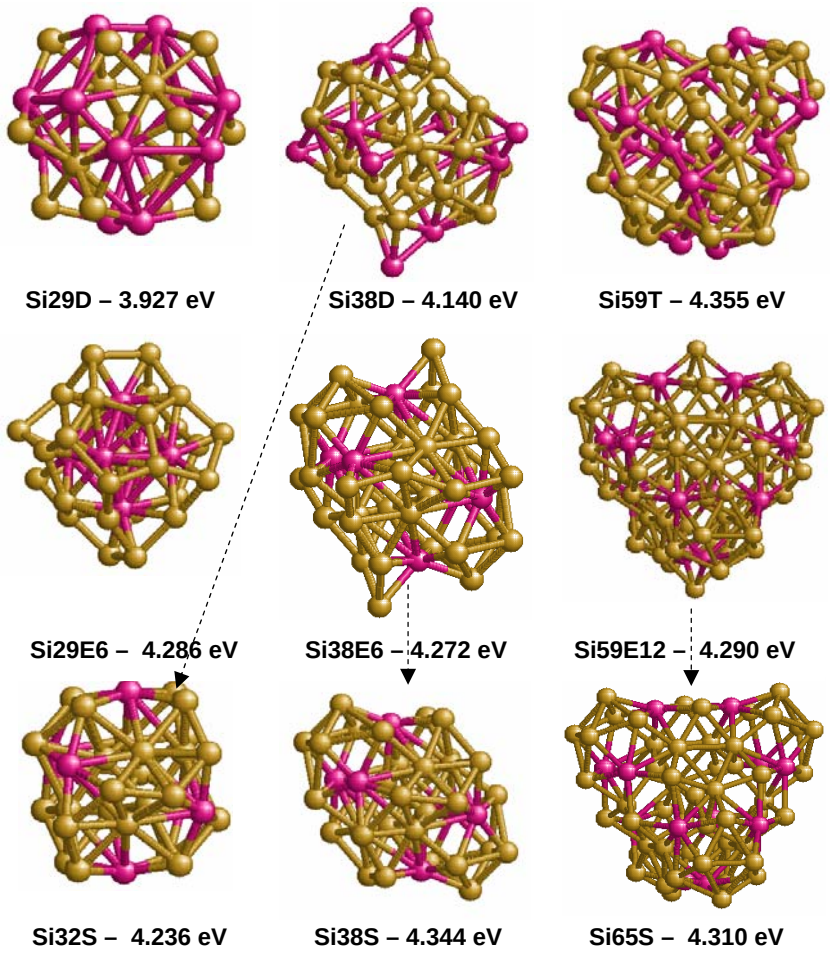


**Figure 5.** (Color online) Optimized geometries of clusters Si29D, Si38D, Si59T, Si29E6, Si38E6, and Si59E12 from Figure 2. Clusters Si32S, Si38S, and Si65S are optimized geometries of clusters that were derived from Si38D, Si38E6, and Si59E12, respectively, by removing 6 vertex atoms in each case to smooth the cluster surface. The cohesive energy per atom for each cluster is also given.

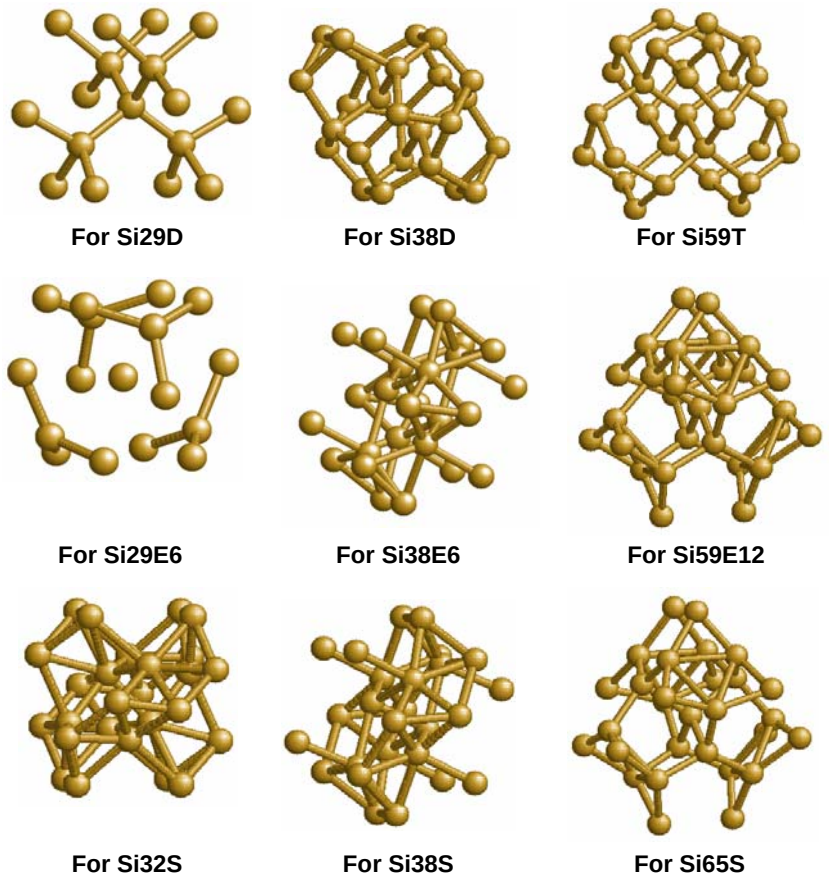


**Figure 6.** (Color online) Clusters from Figure 5 with atoms that were originally on the surface or embedded beneath the surface (pink atoms in Figure 5) removed to identify the final arrangement of the initially diamond-like atoms around the central atom (or the central bond). For the dimerized and trimerized clusters shown in the top row, much of the diamond-like tetrahedral coordination was retained, while for the remaining clusters, most of the diamond-like character was lost in the final geometry.

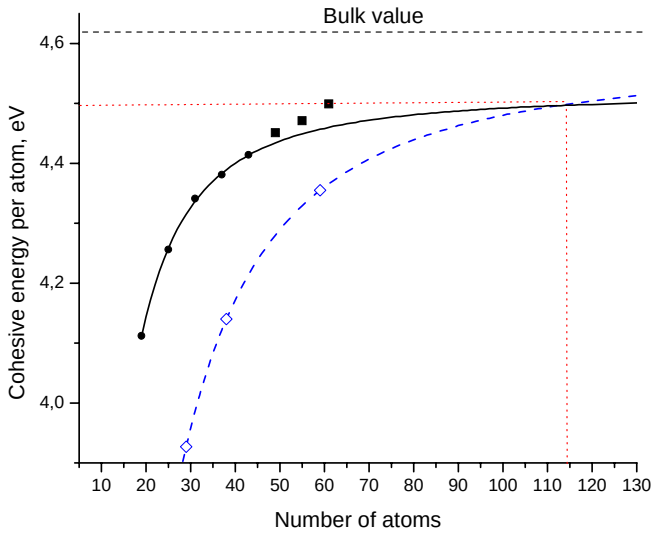


**Figure 7.** (Color online) Cohesive energy per atom for representative non-diamond one-dimensional clusters (black dots) and clusters from the first row of Figure 5 with a diamond-like core (open diamonds). Filled rectangles correspond to clusters with a quasi-two-dimensional end (not used in fitting the curves). The crossing point of the approximating curves represents a lower bound for the transition from non-diamond to diamond-like cluster structure.

Table 1. HOMO-LUMO gaps (eV) of pentagon-based quasi-one-dimensional clusters.

| **Cluster** | Si19 | Si25 | Si31 | Si37 | Si43 | Si49 | Si55 | Si61 |
|---|---|---|---|---|---|---|---|---|
| **HOMO-LUMO gap, eV** | 0.343 | 0.286 | 0.254 | 0.407 | 0.187 | 0.118 | 0.200 | 0.167 |

Table 2. HOMO-LUMO gaps of clusters with originally diamond-like core.

| **Cluster** | **HOMO-LUMO gap, eV** | **Cluster** | **HOMO-LUMO gap, eV** | **Cluster** | **HOMO-LUMO gap, eV** |
|---|---|---|---|---|---|
| Si29D | 0.028 | Si38D | 0.098 | Si59T | 0.166 |
| Si29E6 | 0.523 | Si38E6 | 0.149 | Si59E12 | 0.03 |
| Si32S | 0.217 | Si38S | 0.463 | Si65S | 0.083 |